Vascular Pharmacology 117 (2019) 27–34

Contents lists available at ScienceDirect

Vascular Pharmacology

journal homepage: www.elsevier.com/locate/vph

Vascular angiotensin AT1 receptor neuromodulation in fetal programming of hypertension

M.S. Vieira-Rocha[a,b], P. Rodríguez-Rodríguez[b], J.B. Sousa[a], M.C. González[b], S.M. Arribas[b], A.L. López de Pablo[b], C. Diniz[a,*]

[a] LAQV/REQUIMTE, Laboratory of Pharmacology, Department of Drug Science, Faculty of Pharmacy, University of Porto, Portugal
[b] Department of Physiology, Faculty of Medicine, Universidad Autonoma de Madrid, Spain

ARTICLE INFO

Keywords:
Fetal programming of hypertension
RAS
ANG II
AT1 receptors
Sympathetic nerves

ABSTRACT

Fetal stress increases the susceptibility to cardiovascular diseases in adult age, including hypertension, a process known as fetal programming of hypertension (FPH). This study intends to investigate the interplay between vascular sympathetic nervous system (SNS) and RAS, namely the neuromodulatory role exerted by Angiotensin II (Ang II) receptor-1 (AT1) in FPH, and respective contribution for hypertension.

Methods: 6-month old Sprague-Dawley offspring from mothers fed *ad-libitum* (CONTROL) or with 50% intake during the second half of gestation (maternal undernutrition, MUN) were used. Sympathetic neurotransmission was studied in mesenteric/tail arteries and mesenteric veins by electrically-evoked [^{3}H]-noradrenaline release experiments using RAS drugs. AT1 receptors in sympathetic nerves of mesenteric arteries were investigated by immunohistochemistry and Laser Scanning Confocal Microscopy.

Results: Ang II facilitated noradrenaline release in the vessels studied from MUN and CONTROL rats. Losartan induced a tonic facilitation only in MUN vessels. Sympathetic innervation was larger in MUN versus CONTROL vessels. AT1 receptors on sympathetic nerves were present in higher amounts in MUN versus CONTROL vessels.

Conclusions: Findings support that FPH is associated with a vascular hyper-sympathetic activation, involving a tonic facilitation of prejunctional AT1 receptors by endogenous Ang II, which can justify, at least in part, the development of hypertension.

1. Introduction

Along with genetic and lifestyle factors it is now established that some stress factors during fetal life, particularly undernutrition, contribute to the development, in adult age, of cardiovascular diseases, particularly hypertension [1–8]. This is known as Fetal Programming of Hypertension (FPH). In western countries, although the probability of maternal malnutrition is low, fetal undernutrition may result from placental insufficiency and intrauterine growth retardation, which are increasing due to pregnancy delay.

Several mechanisms have been proposed to explain the relationship between poor fetal growth and later hypertension development. One of the proposed mechanisms is an alteration of the renin angiotensin system (RAS). Thus, in infants with intrauterine growth retardation, renin activity is elevated in umbilical cord and, in animal models of FPH, the pressure response to angiotensin II (Ang II) is elevated [6,9–13]. Indeed, Ang II play a crucial role in blood pressure regulation through pleiotropic actions such as vasoconstriction and vascular/cardiac hypertrophy [14]. These actions of Ang II are mediated via interaction with metabotropic cell membrane bound G-protein coupled receptors. Four types of RAS receptors are known (AT1, AT2, Mas and MrgD), of which the AT1 and AT2 receptors are the most studied. These two receptors share a similar high affinity to Ang II but the consequences of their binding are opposite. AT1 receptor is highly expressed in adults and mediates Ang II-induced vasoconstriction [15], proliferation [16], inflammation [17], and extracellular matrix remodeling [18]. On the other hand, AT2 receptor activation produces opposite effects, providing a cardiovascular protective action [19].

Ang II-induced hypertension is associated with a decrease in cardiac output and a marked increase in total peripheral resistance. Moreover, Ang II has been described to cause increased sympathetic nervous activity in rats consuming a high-salt diet [20]. However, the association between Ang II and sympathetic dysfunction in FPH based on maternal undernutrition is still to be addressed. We postulate that the effects

* Corresponding author at: Faculdade de Farmácia, Departamento de Ciências do Medicamento, Laboratório de Farmacologia, Universidade do Porto, Rua Jorge Viterbo Ferreira n° 228, 4050-047 Porto, Portugal.
E-mail address: cdiniz@ff.up.pt (C. Diniz).

https://doi.org/10.1016/j.vph.2018.10.003
Received 22 June 2018; Received in revised form 31 August 2018; Accepted 12 October 2018
Available online 13 October 2018

mediated by Ang II are altered in FPH individuals leading to an increased vascular sympathetic activity, and consequently, to an increase in vascular responsiveness and hypertension. To check on this possibility, the interplay between SNS and RAS was studied, namely the vascular neuromodulatory role of AT1 receptor in FPH, using an animal model of FPH. We also evaluated the regional distribution/localization and relative amount of AT1 receptors and sympathetic nerves in FPH mesenteric arteries.

2. Materials and methods

2.1. Animals

2.1.1. Animal ethical considerations

Sprague–Dawley (SD) rats from the colony maintained at the animal house facility of the Universidad Autonoma de Madrid were used. All experimental procedures were approved by the Ethics Review Board of Universidad Autonoma de Madrid (CEI63–1112-A097) and conformed to the Guidelines for the Care and Use of Laboratory Animals (National Institutes of Health publication no. 85–23, revised in 1996), the Spanish legislation (RD 1201/2005) and the Directive 2010/63/EU on the protection of animals used for scientific purposes. The rats were housed in buckets 36.5/21.5/18.5 cm (length/width/height) on aspen wood bedding, under controlled conditions of 22 °C, 40% relative humidity and 12/12 light/dark photoperiod. The animal health monitoring indicated that they were free from pathogens that may interact with any of the parameters studied. The rats were fed with breeding diet (SAFE A03) containing 51.7% carbohydrates, 21.4% protein, 5.1% lipids, 3.9% fiber, 5.7% minerals and 12.2% humidity (Safe Augy, France). Drinking water was provided *ad libitum* in all cases.

2.1.2. Experimental animal model of FPH

FPH model based on global maternal nutrient restriction was induced as previously described [21]. The litters were divided in two groups, one from mothers receiving *ad libitum* diet (CONTROL) throughout pregnancy and the other group from mothers with *ad libitum* diet during the first 10 days of gestation and 50% of the daily intake from day 11 to the end of gestation (Maternal Undernutrition, MUN). The maximum daily intake of rat chow was previously determined in a group of pregnant rats as 24 g/day. Therefore, during the second half of gestation, the second group received 12 g of rat chow per day. After delivery the litters were culled to 12 rats and the respective mothers received food *ad libitum* during the suckling period. 6 month old male offspring from MUN (n = 6) and CONTROL (n = 6) were used. The animals were euthanized using a guillotine, the method reported as the sacrificial advisable in studies involving the nervous system. The mesenteric and tail arteries and the mesenteric vein were collected and immediately used. Four segments were obtained from each vessel for different experimental procedures.

2.2. Chemicals

The following drugs were used: levo-[ring-2,5,6-3H]-noradrenaline, specific activity 44.8 Ci/mmol (DuPont NEN, I.L.C., Lisboa, Portugal), losartan (Merck Portuguesa, Lisbon, Portugal), angiotensin II (Sigma-Aldrich, St. Louis, USA) and desipramine hydrochloride purchased from Sigma-Aldrich (Sintra, Portugal). The following antibodies were used: rabbit polyclonal anti-AT1 were purchased from Santa Cruz Biotechnology, Inc., CA, USA and mouse monoclonal anti-tyrosine hydroxilase antibody (TH, ab129991,Abcam, UK) and mouse monoclonal anti-glial fribrilary acidic protein (GFAP, G6171, Sigma-Aldrich, Inc., USA). The following fluorescent probes were used: Alexa Fluor 488 goat anti-mouse IgG (H + L) antibody, highly cross-adsorbed and Alexa Fluor 647 goat anti-rabbit IgG (H + L) antibody, highly cross-adsorbed (Molecular Probes) secondary fluorescent antibodies (Invitrogen, Life Technologies, SA, Madrid, Spain); vectashield mounting medium with DAPI (Vector Laboratories, UK). Stock solutions were made up in ultrapure water and diluted in superfusion medium immediately before use.

2.3. Hemodynamic parameters measurement

Systolic blood pressure (SBP) was measured using the tail-cuff method with a NIPREM 645 noninvasive blood pressure acquisition system for rats (CIBERTEC, Madrid, Spain). The experiments were conducted in a quiet area at 22 ± 2 °C. Firstly, the rats were placed in a chamber at 37 °C for 10–15 min to induce vasodilatation. Thereafter, they were placed inside a soft support in the darkness to prevent excessive movement. A pulse sensor and a pressure cuff were place around the tail for SBP recordings. Sessions of recorded measurements were all made by a single investigator. The cuff was inflated to 150 mmHg and 15 to 25 pressure inflate-deflate cycles were performed and data were automatically registered. The first 5 cycles were considered “acclimatization” cycles and were not used in the analysis. This procedure was obtained during 3 consecutive days for the rats to become accustomed. The measurements recorded on days 2 and 3 were similar and averaged for statistical analysis.

2.4. [^{3}H]-Noradrenaline release experiments

[^{3}H]-noradrenaline release experiments were carried out as previously described [27–29]. Vessels were preincubated in 2 mL Krebs-Henseleit solution (KHS) containing 0.1 μmol/L [^{3}H]-noradrenaline (for 60 min at 37 °C) and transferred into superfusion chambers, superfused with [^{3}H]-noradrenaline-free KHS (1 mL/min; constant rate) with desipramine 400 nmol/L to inhibit noradrenaline's neuronal uptake. After 30 min of stabilization, two periods of electrical stimulation (5 Hz, 100 pulses, 1 ms, 50 mA; Hugo Sachs Elektronik, March-Hugstetten, Germany) were applied, S_1 and S_2, with 30 min intervals (t = 90 min and t = 120 min, respectively). The superfusate was collected each 5 min period from 85 min of superfusion onwards.

To address the implication of presynaptic AT1 receptors, the agonist for AT1 receptors, Ang II (30 nmol/L), and the antagonist, losartan (100 nmol/L), were used: Ang II was added 5 min before S_2 and was present until the end of the stimulation period; losartan was added immediately after S_1 and kept until the end of the experiment.

At the end of the experiments (t = 130 min), the tritium was measured in the collected superfusate samples and in the vessels (previously solubilized: sonicated 1 h with 2.5 mL, 0.2 mol/L perchloric acid). For this, 6 mL of a scintillation mixture (OptiPhase ‘Hisafe’ 3, PerkinElmer, I.L.C., Lisboa, Portugal) was added to each sample and analyzed by liquid scintillation spectrometry (LS 6500, Beckman Instruments, Fullerton, USA).

2.4.1. Measurement of drug effects on electrically-evoked tritium overflow

Tissue labelling with [^{3}H]-noradrenaline and evaluation of electrically-evoked tritium overflow changes was performed as previously described [22,23]. Effects of drugs added after S_1 on electrically-evoked tritium overflow were evaluated as ratios of the overflow elicited by S_2 and the overflow elicited by S_1 (S_2/S_1). S_2/S_1 ratios obtained in individual experiments in which a drug was added after S_1 were calculated as a percentage of the respective mean ratio in the appropriate control group (solvent instead of the respective drug).

2.5. Laser scanning confocal microscopy (LSCM) experiments

Immunohistochemistry procedures were previously described [26]. Briefly, the artery was immediately placed in cold phosphate buffer solution (PBS; in g/L): NaCl 8.0, $Na_2HPO_4.2H_2O$ 0.77, KCl 0.20, KH_2PO_4 0.19 (pH 7.2), and was cut in 4 segments. Each artery segment was longitudinally opened and fixed (paraformaldehyde 4% PBS; 50 min; room temperature). After two 15 min PBS washing cycles,

artery segments were incubated with primary antibodies raised against rabbit polyclonal angiotensin receptor subtype anti-AT1 (AT1, 1:100 dilution, overnight, 4 °C) and mouse monoclonal anti-tyrosine hydroxylase (TH, 1:100 dilution, overnight, 4 °C) to stain noradrenergic nerve terminals or mouse monoclonal anti-glial fibrillary acidic protein (GFAP, 1:200 dilution, overnight, 4 °C) to stain glial cells such as Schwann cells. Thereafter, tissues were incubated with Alexa 647 anti-rabbit and Alexa 488 anti-mouse fluorescent secondary antibodies (1:1000 dilution, 1 h, room temperature). Negative controls were incubated on adjacent sections using 10% normal horse serum or blocking solution instead of the primary antibody. After two PBS washing cycles, tissue preparations were mounted with antifading agent (vectashield mounting medium with DAPI, Vector Laboratories, UK), with the adventitial side facing up. Preparations were visualized with a Leica SP5 LSCM system (Leica Microsystems, Wetzlar, Germany) fitted with an inverted microscope (× 63 oil immersion lens). Stacks of 1-μm-thick serial optical images were captured from the entire adventitial layer, which was identified by the shape and orientation of the nuclei stained with DAPI [30].

From each preparation, three stacks of images were sequentially obtained from the same region, the first with the Ex 405 nm and Em 412–470 nm wavelength to visualize cell nuclei. The second was taken with the Ex 488 nm and Em 490–570 nm wavelength to visualize the TH or GFAP staining (location of noradrenergic terminals or glial cells) and the third with the Ex 633 nm and Em 640–720 nm wavelength, to detect the AT1 receptor distribution stained with the secondary antibody Alexa Fluor 647 (different subtypes depending on primary antibody). Image acquisition was performed always under the same laser power, brightness, and contrast conditions. Adventitia was scanned along each mesenteric artery segment and the resulting images were reconstructed separately for each wavelength.

2.5.1. Specificity of primary antibodies

The specificity of the primary AT1 antibody used has been established in previous studies: AT1 sc-31,181 [24,25]. In addition, pre-adsorption with the corresponding synthetic peptide antigen was carried out in our experimental conditions for all the primary antibodies used. Western-blot was also performed using arteries extracts as protein source to immunoblot with antibodies and/or with peptides.

2.5.2. Laser scanning confocal microscopy images quantification

Quantitative analysis of confocal z-stacks images was performed using image analysis software (PAQI, CEMUP, Porto, Portugal), as previously described [22,26]. Briefly, a sequential routine was designed and developed to analyze each fluorescent signal used. PAQI software measured the surface area and strength of the fluorescence signal marking the postganglionic nerves, the surface area and strength of the fluorescence signal marking the receptors and determined the surface area of attachment of the receptors on the nerves as well as the intensity of fluorescence of the receptors on nerves (corrected for background).

2.6. Data analysis

Results are expressed as mean ± s.e.m. and n denotes the number of animals used. Quantitative analysis of confocal images is presented as staining fractional area, expressed as a percentage of the tissue total area. Differences of means were compared for significance using one- or two-way ANOVA, followed by post-hoc Holm-Sidak's multicomparison *t*-test or Student's *t*-test. A P value lower than 0.05 was considered to denote statistically significant differences.

3. Results

3.1. Blood pressure measurements

Blood pressure was evaluated in MUN and CONTROL animals: a significantly larger SBP values were observed in MUN (164.40 ± 3.61 mmHg; n = 6) comparatively to values from CONTROL animals (134.13 ± 3.35 mmHg, respectively; n = 6; p = .003).

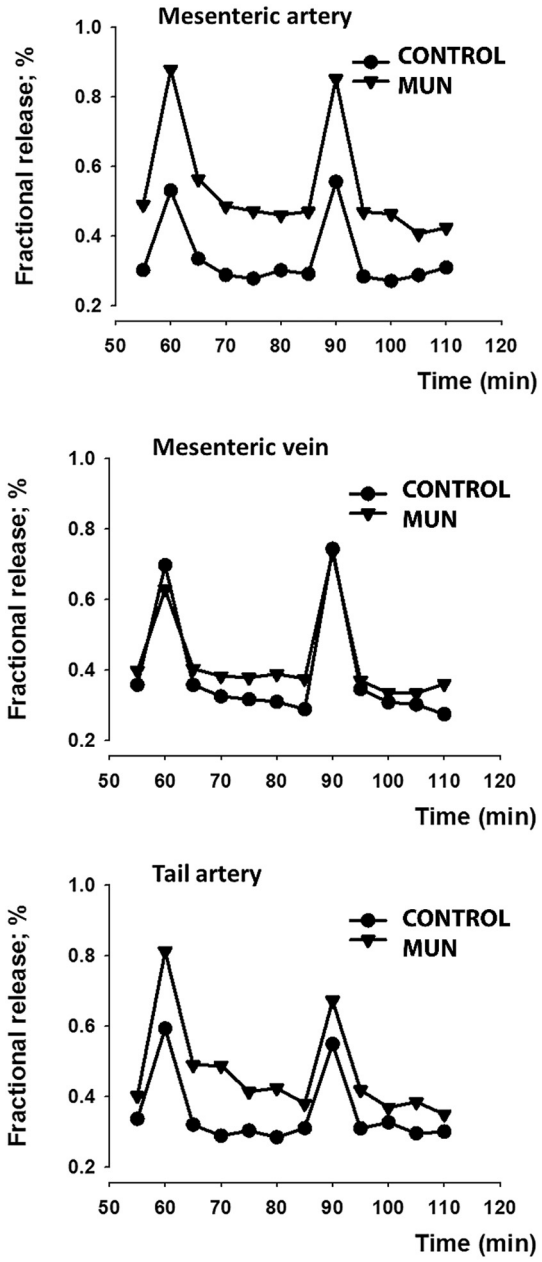

Fig. 1. Representative examples of time course tritium outflow from: mesenteric artery, mesenteric vein and tail artery from CONTROL (circles) and MUN (triangles) from typical experiments. After pre-incubation with [^{3}H]-noradrenaline, tissues were superfused with [^{3}H]-noradrenaline free medium containing desipramine (400 nM). Tritium outflow (ordinates) is expressed as a percentage of the total radioactivity present in the tissue at the beginning of the collection period and was measured in samples collected every 5 min. Artery segments were stimulated twice by 100 pulses/5 Hz, (S_1, S_2). Each line represents the outflow of tritium from a single superfusion chamber.

3.2. Noradrenaline release from sympathetic nerve terminals

Electrically-evoked tritium overflow from tissue preparations incubated with [^{3}H]-noradrenaline has been shown to reflect action potential-evoked neuronal noradrenaline release and drug-induced

Table 1
Basal tritium outflow (b_1), electrically evoked tritium overflow (S_1) and S_2/S_1 ratios from SD-C and SD-MUN vessels.

	Basal outflow (b_1) (fractional rate of outflow; min^{-1})	Evoked overflow (S_1) (% of tissue tritium content)	S_2/S_1	n
Mesenteric artery				
SD-C	0.097 ± 0.009	0.221 ± 0.039	1.085 ± 0.091	7
SD-MUN	0.093 ± 0.007	0.348 ± 0.029*	1.076 ± 0.009	5
Mesentery vein				
SD-C	0.088 ± 0.006	0.265 ± 0.021	0.992 ± 0.057	7
SD-MUN	0.073 ± 0.006	0.381 ± 0.032*	1.078 ± 0.068	5
Tail artery				
SD-C	0.072 ± 0.007	0.163 ± 0.045	1.001 ± 0.098	7
SD-MUN	0.082 ± 0.009	0.268 ± 0.003*	1.086 ± 0.089	5

changes in evoked tritium overflow can be assumed to reflect changes in neuronal noradrenaline release, as observed in previous studies [22,26,27].

Electrical field stimulation (100 pulses/5 Hz) significantly increased tritium outflow from all vessels studied of both CONTROL and MUN rats (Fig. 1). The fractional rate of basal tritium outflow (b_1), electrically-evoked tritium overflow (S_1) of mesenteric arteries and veins and of tail arteries are shown in Table 1. Basal outflow and electrically-evoked tritium overflow remained constant throughout the CONTROL experiments, with b_n/b_1 and S_n/S_1 values close to unity. Electrically-evoked tritium overflow (S_1) was higher in MUN compared to CONTROL vessels (Table 1).

Tissue preparations of mesenteric and caudal arteries and mesenteric vein were pre-incubated with [^{3}H]-noradrenaline for 40 min. After pre-incubation with [^{3}H]-noradrenaline, tissues were superfused with [^{3}H]-noradrenaline free medium containing desipramine (400 nM). Tissues were stimulated twice at 30-min intervals (S_1-S_2; 100 pulses, 5 Hz, 1 ms, 50 mA): b_1 refers to the 5-min period immediately before S_1. The electrically-evoked tritium overflow was calculated by subtracting the estimated basal outflow from total outflow observed during and in the 25-min period subsequent to S_1 and expressed as a percentage of the tissue tritium content at the onset of stimulation. Values presented are means ± SEM and n denotes the number of tissue preparations. Significant differences of S_1 values from SD-C vessels: *P < 0.05.

3.3. Role of Ang II in vascular sympathetic neurotransmission

Ang II (30 nmol/L; a non-selective agonist of angiotensin receptors) facilitated electrically-evoked tritium overflow in all the vessels studied from both experimental groups, as shown by the ratio (S_2/S_1) in the absence of the drug. No statistical differences were observed between different vessels or between different experimental groups (Fig. 2), indicating that exogenous activation of angiotensin receptors is equivalent in arteries and veins and was not modified by maternal undernutrition.

Endogenous Ang II-mediated effects in vascular sympathetic neurotransmission were evaluated by blocking the AT1 receptor with a selective antagonist. In the presence of the AT1 receptor antagonist losartan (100 nmol/L), an inhibition of electrically-evoked tritium overflow was observed in all the MUN vessels studied (Fig. 2). Losartan was unable to modify tritium overflow in vessels from CONTROL rats. This finding is consistent with the occurrence of a tonic facilitation mediated by endogenous Ang II via AT1 receptor activation in MUN rats.

3.4. Localization of AT1 receptors adventitia mesenteric arteries

Adventitial layer of mesenteric arteries was identified from LSCM

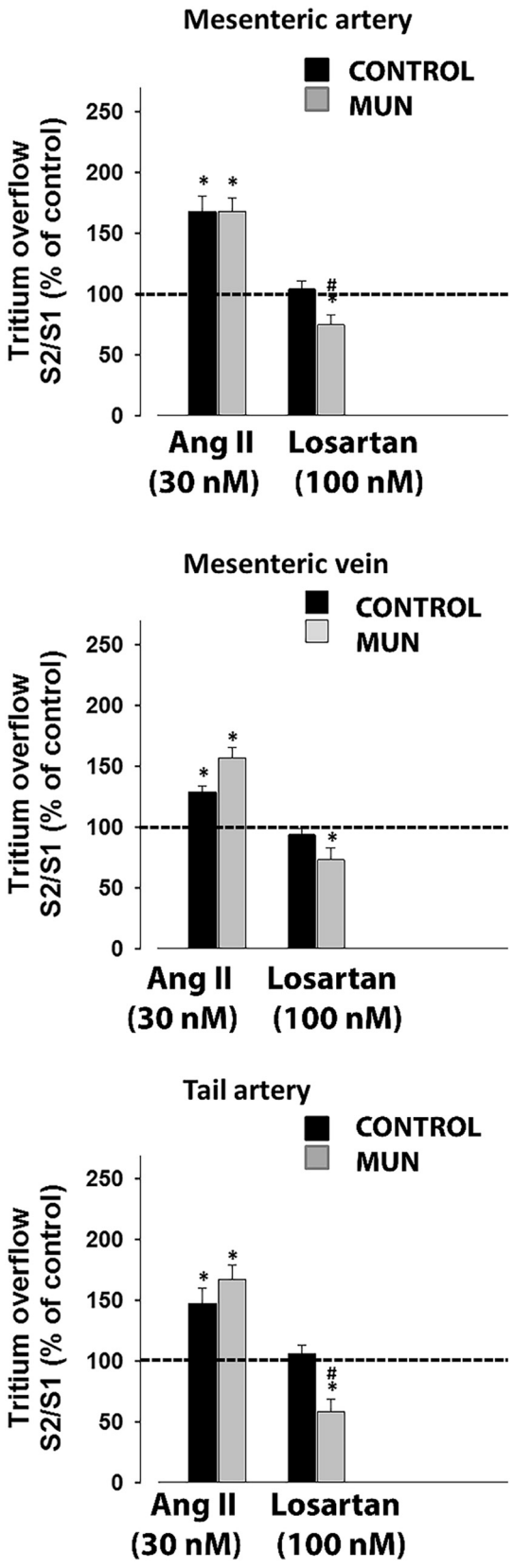

Fig. 2. Effects of Ang II (30 nM) or of losartan (100 nM) on the electrically-evoked tritium overflow from CONTROL and MUN vessels. Ang II was added 10 min before S_2 and was present until the end of the stimulation period. Losartan was added immediately after S_1 and kept until the end of the experiment. Ordinates: S_2/S_1 values obtained in individual tissue preparations, expressed as a percentage of the appropriate S_2/S_1 CONTROL value. Values are mean ± s.e.m. from 5 to 16 tissue preparations. Significant differences from the appropriate CONTROL: *P < 0.05; from the CONTROL vessels: #P < 0.05.

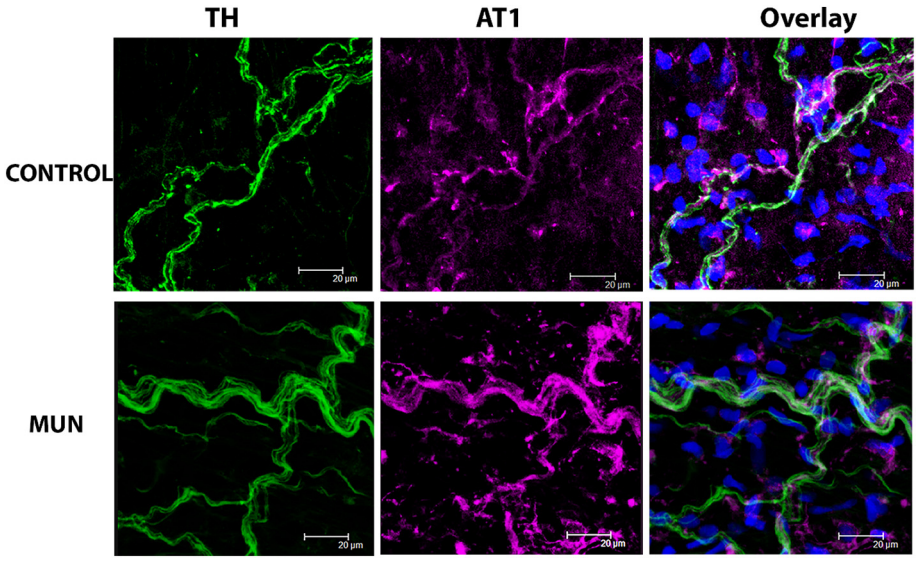

Fig. 3. Laser scanning confocal microscopy representative images of CONTROL and MUN mesenteric arteries exhibiting TH (green), AT1 receptor (red), and overlay of AT1 receptor-TH immunoreactivities; nuclei are shown in blue. Scale bar = 20 µm. (For interpretation of the references to colour in this figure legend, the reader is referred to the web version of this article.)

images by the shape and orientation of the nuclei [28]. No significant immunoreactivity was observed when the primary antibodies were omitted (negative controls; Supplementary material). Immunoreactivity for the sympathetic neuronal marker TH was evident in mesenteric arteries from both experimental groups (Fig. 3, green images). MUN vessels exhibited a larger immunoreactivity compared to CONTROL arteries.

LSCM also revealed the presence of AT1 immunoreactivity in both CONTROL and MUN mesenteric arteries (Fig. 3, red images). Quantitative analysis evidenced that the relative amount of AT1 immunoreactivity present in MUN arteries was much higher (up to 80% higher) than that exhibited by CONTROL vessels (Fig. 4A). These results together with functional data (Fig. 2) reveal and support differences in the sympathetic dynamic induced by AT1 receptors in MUN animals. It is relevant to notice the absence of a pattern compatible with a co-localization of TH with AT1 receptors immunoreactivities. This is in line with previous reports using this sympathetic neuronal marker and other membrane receptors [22,23] and, it is explained by the fact that AT1 receptors is present at the cytoplasmatic membrane while the enzyme tyrosine hydroxylase is storage inside vesicles in the sympathetic axoplasm [29]. Immunoreactivity for AT1 receptors show substantial overlay with TH marker suggesting that these receptors might be localized on the same structure, the postganglionic sympathetic nerves. Nonetheless, immunoreactivity for AT1 receptors in non-neuronal cells could also be observed.

Quantitative analysis of LSCM images revealed considerable differences in the relative mean of TH, AT1 and AT1-TH overlay between the two experimental animal groups (Fig. 4A): values obtained from MUN animals almost doubled comparatively to CONTROL.

Relative mean ratio of AT1 receptor and TH overlay, with respect to the total TH immunoreactivity, was slightly higher in MUN comparatively to CONTROL mesenteric arteries: 25% of sympathetic neurons exhibit AT1 receptor immunoreactivity in CONTROL versus 35% observed in MUN vessels (Fig. 4B). Also, the relative mean ratio of AT1 receptor and TH overlaid, regarding the total AT1 immunoreactivity revealed the presence of AT1 receptors in other cells than sympathetic neurons: 70% in CONTROL and 60% in MUN mesenteric arteries (Figs. 3 and 4C).

We have previously demonstrated that sympathetic nerves are surrounded by Schwann cells (anti-GFAP-immunoreactivity) [30]. The putative presence of AT1 receptors in Schwann cells was evaluated staining vessels with GFAP. Data from LSCM images evidenced the occurrence of AT1 and GFAP overlaid immunoreactivities (Fig. 5), confirming the presence AT1 receptors in adventitia cells other than the postganglionic sympathetic neurons.

4. Discussion

There is a gap in the knowledge regarding the complex interplay between vascular sympathetic neurotransmission and Ang II in FPH. This study points out that an increase vascular sympathetic activity might play an important role on hypertension development subsequent to fetal undernutrition. This is a relevant finding since sympathetic nervous system is a key contributor to vascular tone. Therefore, an increase in sympathetic neurotransmission would, likely, lead to an elevation in vascular resistance and subsequent elevation of blood pressure.

In MUN male rats a significant elevation in SBP was observed. This data in conscious rats is similar to that previously reported in male offspring from this rat model under anesthesia [31].

An increase in sympathetic neurotransmission was observed in our model of FPH both in arterial and venous territories. This data is in accordance with studies previously performed in a spontaneously hypertensive rat model, the SHR, where a hyper-sympathetic activity was also described in several arterial territories such as cerebral [32,33], tail [26] and mesenteric [26,27] and also in mesenteric vein [27]. Moreover, data is also in agreement with studies demonstrating that sympathetic nervous system activation seem to be increased in other models of FPH [34,35]. Some of these studies reported an increased circulating levels of noradrenaline: a model of intrauterine growth restriction induced by maternal protein restriction in the rat [36] and another model of placental insufficiency in both rat [37] and sheep [38,39]. In addition, chronic prenatal hypoxia is associated with hyperinnervation and an increase in adrenal medullary noradrenaline content and TH activity [40–42]. Therefore, and in accordance with those reported data, our findings indicate that the hyper-sympathetic activity observed in MUN vascular tissues can be explained by the larger amount of sympathetic innervation, as demonstrated by TH staining.

In MUN vessels, the observed increase in basal and electrically-induced noradrenaline release seems to be more evident in arteries than in veins. This data also suggests that the baseline tone is higher in arteries from MUN than in CONTROL. In fact, noradrenaline once released can activate α_1-adrenoceptors in vascular smooth muscle cells leading to vasoconstriction in arteries [43,44] and in veins [45,46] as noticed on splanchnic circulation and other vascular territories in animal models of hypertension.

We also observed that release of noradrenaline from sympathetic

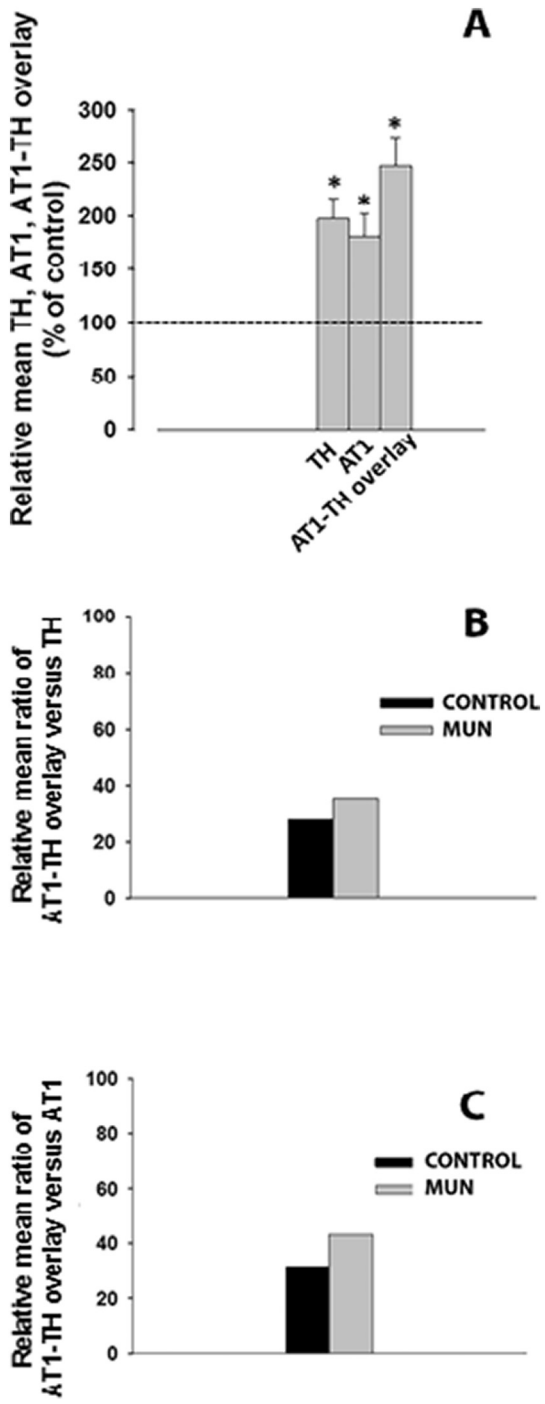

Fig. 4. Quantitative analysis of LSCM images from mesenteric arteries (CONTROL and MUN) staining with TH and AT1 antibodies. (A) Relative means of TH, AT1 and TH-AT1 overlay expressed as percentage of CONTROL values; (B) Mean percentage of overlay ratio with TH (C) and mean percentage of overlay ratio with AT1 are depicted. Images are reconstructions from 9 to 28 serial optical sections analyzed using PAQI software. Values are mean ± s.e.m., and n = 3–4 animals. Significant differences from SD-CONTROL: *P < 0.05.

nerve terminals was under the influence of Ang II through AT1 receptors. Thus, exogenous Ang II caused an increase in noradrenaline release both in arteries and veins from CONTROL and MUN groups, confirming the interplay between RAS and vascular neurotransmission. The facilitatory role of Ang II on noradrenaline release has been previously demonstrated in rat models of hypertension [47–50] other than FPH. In this study, the facilitation of noradrenaline release induced by exogenous Ang II was more pronounced in the arterial territories than in the veins from CONTROL animals. In addition, exogenous Ang II caused a similar increase in noradrenaline release in CONTROL and MUN but only in the arterial tissues. In the mesenteric veins, the facilitation of noradrenaline release was more marked in MUN than in CONTROL veins. These findings are in line with results obtained in other studies made in mesenteric veins of SHR animals [51].

It has been shown that inappropriate activation of the RAS may occur in response to a development insult: prenatal exposure to glucocorticoids up-regulates expression of the renal RAS [52]; central expression of the AT1 receptors is increased in offspring exposed to maternal protein restriction [53] and nicotine exposure [54]. However, in a maternal undernutrition animal model, these alterations had not been studied.

In our study, the treatment with AT1 receptor antagonist losartan was unable to modify tritium overflow in vessels from CONTROL rats. However, this procedure caused a facilitation in MUN vessels. This finding is consistent with the occurrence of a tonic facilitation mediated by endogenous Ang II via AT1 receptor activation. This effect was observed in all the MUN vessels studied.

Data support the possible occurrence of higher levels of endogenous Ang II in the sympathetic cleft of MUN rats. Curiously, the tonic effect, mediate by endogenous Ang II in prejuctional AT1 receptors was similar in all the MUN vessels studied, discarding the possibility that this vascular sympathetic alteration occurs only locally or in specific territories, but rather indicating a widespread effect both in resistance and capacitance vessels.

Taken together data revealed that local RAS is more effective in vascular sympathetic neurotransmission modulation in arterial territories than in veins. Furthermore, it also reinforces their relevance as a potential mechanism in FPH.

Since all the vessels studied showed a similar functional profile in vascular neurotransmission we chose the mesenteric artery as a representative vessel for the morphological study. LSCM data revealed the presence of nerve fibers (TH positive) both in CONTROL and MUN. We observed that sympathetic nerves spread through the adventitia reaching the medial layer. There was, however, a larger thickness of sympathetic nerve fibers in MUN mesenteric arteries accompanied by a parallel AT1 receptors overlaying these neurons. These higher amounts of AT1 receptors can explain, at least in part, the facilitatory tone regulating noradrenaline release from MUN mesenteric arteries stimulated with exogenous or endogenous Ang II. Data also show for the first time that AT1 are located in two main locations: one expressed in nerve fibers and another, in other adventitia cells. Some of these cells seem to be Schwann cells. This possibility was confirmed by data showing that AT1 receptors are overlaying GFAP, a marker for glial cells such as Schwann cells. In fact, the presence in Schwann cells, of other receptors or enzymes with a role on noradrenaline neurotransmission, was previously demonstrated [22,26] supporting a trophic role of these cells and of its close association with neurons. Images also show that these receptors are present in other type of adventitia cells like macrophages or mesenchymal cells. Altogether these data correlates well with the functional results obtained, showing an increase in the neuromodulatory role ascribed to Ang II in several vascular beds.

In summary, this study supports the occurrence of a hyper-sympathetic activation, involving a tonic facilitation, by endogenous Ang II, of prejunctional AT1 receptors, which can justify, at least in part, the occurrence of hypertension in these animals. These alterations also supports the possibility of vascular remodeling in MUN mesenteric arteries, as previously described in aorta [55]. A vascular structural alteration could also contribute to increase vascular resistance and the development of hypertension in this model of FPH.

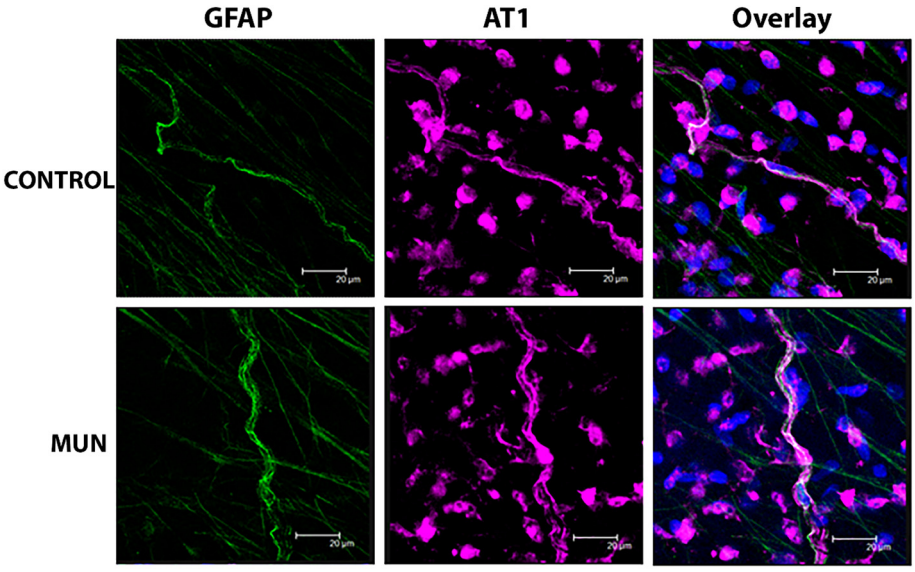

Fig. 5. Laser scanning confocal microscopy representative images of CONTROL and MUN mesenteric arteries exhibiting GFAP (green), AT1 receptor (red), and overlay of AT1-GFAP immunoreactivities, nuclei (blue). Scale bar = 20 μm. (For interpretation of the references to colour in this figure legend, the reader is referred to the web version of this article.)

Acknowledgments

This work received financial support from Fundação para a Ciência e Tecnologia (FCT), Portugal through project UID/QUI/50006/2013 - POCI/01/0145/FEDER/007265 with financial support from FCT/MEC through national funds and co-financed by FEDER, under the Partnership Agreement PT2020 and Ministerio de Economia y Competitividad (FEM2015-63631-R, Spain).

Appendix A. Supplementary data

Supplementary data to this article can be found online at https://doi.org/10.1016/j.vph.2018.10.003.

References

[1] A. Forsdahl, Are poor living conditions in childhood and adolescence an important risk factor for arteriosclerotic heart disease? Br. J. Prev. Soc. Med. 31 (2) (1977) 91–95.
[2] D.J. Barker, Intrauterine programming of coronary heart disease and stroke, Acta Paediatr. Suppl. 423 (1997) 178–182 (discussion 83).
[3] D.J. Barker, C. Osmond, Childhood respiratory infection and adult chronic bronchitis in England and Wales, Br. Med. J. (Clin. Res. Ed.) 293 (6557) (1986) 1271–1275.
[4] D.J. Barker, P.M. Clark, Fetal undernutrition and disease in later life, Rev. Reprod. 2 (2) (1997) 105–112.
[5] P.D. Gluckman, M.A. Hanson, Developmental and epigenetic pathways to obesity: an evolutionary-developmental perspective, Int. J. Obes. 32 (Suppl. 7) (2008) S62–S71.
[6] A.M. Nuyt, Mechanisms underlying developmental programming of elevated blood pressure and vascular dysfunction: evidence from human studies and experimental animal models, Clin. Sci. (Lond.) 114 (1) (2008) 1–17.
[7] A.F. Van Abeelen, M.V. Veenendaal, R.C. Painter, S.R. De Rooij, S. Thangaratinam, J.A. Van Der Post, et al., The fetal origins of hypertension: a systematic review and meta-analysis of the evidence from animal experiments of maternal undernutrition, J. Hypertens. 30 (12) (2012) 2255–2267.
[8] I.C. McMillen, J.S. Robinson, Developmental origins of the metabolic syndrome: prediction, plasticity, and programming, Physiol. Rev. 85 (2) (2005) 571–633.
[9] L. Poston, N. Igosheva, H.D. Mistry, P.T. Seed, A.H. Shennan, S. Rana, et al., Role of oxidative stress and antioxidant supplementation in pregnancy disorders, Am. J. Clin. Nutr. 94 (6 Suppl) (2011) 1980S–1985S.
[10] K. Tamura, K. Ohki, R. Kobayashi, K. Uneda, K. Azushima, M. Ohsawa, et al., Fetal programming by high-sucrose diet during pregnancy affects the vascular angiotensin II receptor-PKC-L-type Ca(2+) channels (Cav1.2) axis to enhance pressor responses, Hypertens. Res. 37 (9) (2014) 796–798.
[11] V.M. Vehaskari, T. Stewart, D. Lafont, C. Soyez, D. Seth, J. Manning, Kidney angiotensin and angiotensin receptor expression in prenatally programmed hypertension, Am. J. Physiol. Renal Physiol. 287 (2) (2004) F262–F267.
[12] A.C. Marshall, H.A. Shaltout, N.T. Pirro, J.C. Rose, D.I. Diz, M.C. Chappell, Enhanced activity of an angiotensin-(1-7) neuropeptidase in glucocorticoid-induced fetal programming, Peptides 52 (2014) 74–81.
[13] P. Gonzalez-Rodriguez Jr., W. Tong, Q. Xue, Y. Li, S. Hu, L. Zhang, Fetal hypoxia results in programming of aberrant angiotensin ii receptor expression patterns and kidney development, Int. J. Med. Sci. 10 (5) (2013) 532–538.
[14] M. de Gasparo, New basic science initiatives with the angiotensin II receptor blocker valsartan, J. Renin-Angiotensin-Aldosterone Syst. 1 (2 Suppl) (2000) S3–S5.
[15] R.M. Touyz, The role of angiotensin II in regulating vascular structural and functional changes in hypertension, Curr. Hypertens. Rep. 5 (2) (2003) 155–164.
[16] P. Schelling, H. Fischer, D. Ganten, Angiotensin and cell growth: a link to cardiovascular hypertrophy? J. Hypertens. 9 (1) (1991) 3-15.
[17] R.M. Touyz, F. Tabet, E.L. Schiffrin, Redox-dependent signalling by angiotensin II and vascular remodelling in hypertension, Clin. Exp. Pharmacol. Physiol. 30 (11) (2003) 860–866.
[18] P.J. Lijnen, V.V. Petrov, R.H. Fagard, Angiotensin II-induced stimulation of collagen secretion and production in cardiac fibroblasts is mediated via angiotensin II subtype 1 receptors, J. Renin-Angiotensin-Aldosterone Syst. 2 (2) (2001) 117–122.
[19] R.M. Carey, Newly discovered components and actions of the renin-angiotensin system, Hypertension 62 (5) (2013) 818–822.
[20] J.W. Osborn, G.D. Fink, Region-specific changes in sympathetic nerve activity in angiotensin II-salt hypertension in the rat, Exp. Physiol. 95 (1) (2010) 61–68.
[21] D. Munoz-Valverde, P. Rodriguez-Rodriguez, P.Y. Gutierrez-Arzapalo, A.L. Lopez De Pablo, M. Carmen Gonzalez, R. Lopez-Gimenez, et al., Effect of fetal undernutrition and postnatal overfeeding on rat adipose tissue and organ growth at early stages of postnatal development, Physiol. Res. 64 (4) (2015) 547–559.
[22] J.B. Sousa, M.S. Vieira-Rocha, C. Sa, F. Ferreirinha, P. Correia-De-Sa, P. Fresco, et al., Lack of endogenous adenosine tonus on sympathetic neurotransmission in spontaneously hypertensive rat mesenteric artery, PLoS One 9 (8) (2014) e105540.
[23] C. Rocha-Pereira, S.M. Arribas, P. Fresco, M.C. Gonzalez, J. Goncalves, C. Diniz, Impaired inhibitory function of presynaptic A1-adenosine receptors in SHR mesenteric arteries, J. Pharmacol. Sci. 122 (2) (2013) 59–70.
[24] M.E. Giles, R.T. Fernley, Y. Nakamura, I. Moeller, G.P. Aldred, T. Ferraro, et al., Characterization of a specific antibody to the rat angiotensin II AT1 receptor, J. Histochem. Cytochem. 47 (4) (1999) 507–516.
[25] B. Villar-Cheda, M.A. Costa-Besada, R. Valenzuela, E. Perez-Costas, M. Melendez-Ferro, J.L. Labandeira-Garcia, The intracellular angiotensin system buffers deleterious effects of the extracellular paracrine system, Cell Death Dis. 8 (9) (2017) e3044.
[26] J.B. Sousa, M.S. Vieira-Rocha, S.M. Arribas, M.C. Gonzalez, P. Fresco, C. Diniz, Endothelial and neuronal nitric oxide activate distinct pathways on sympathetic neurotransmission in rat tail and mesenteric arteries, PLoS One 10 (6) (2015) e0129224.
[27] C. Rocha-Pereira, J.B. Sousa, M.S. Vieira-Rocha, P. Fresco, J. Goncalves, C. Diniz, Differential inhibition of noradrenaline release mediated by inhibitory A(1)-adenosine receptors in the mesenteric vein and artery from normotensive and hypertensive rats, Neurochem. Int. 62 (4) (2013) 399–405.
[28] S.M. Arribas, C. Hillier, C. Gonzalez, S. McGrory, A.F. Dominiczak, J.C. McGrath, Cellular aspects of vascular remodeling in hypertension revealed by confocal microscopy, Hypertension 30 (6) (1997) 1455–1464.
[29] H. Bonisch, M. Bruss, The norepinephrine transporter in physiology and disease, Handb. Exp. Pharmacol. 175 (2006) 485–524.
[30] J.B. Sousa, P. Fresco, C. Diniz, Endothelial dysfunction impairs vascular neurotransmission in tail arteries, Neurochem. Int. 80 (2015) 7–13.
[31] P. Rodriguez-Rodriguez, A.L. Lopez De Pablo, C.F. Garcia-Prieto, B. Somoza, B. Quintana-Villamandos, J.J. Gomez De Diego, et al., Long term effects of fetal undernutrition on rat heart. Role of hypertension and oxidative stress, PLoS One 12 (2) (2017) e0171544.
[32] K.S. Butcher, V.C. Hachinski, J.X. Wilson, C. Guiraudon, D.F. Cechetto, Cardiac and sympathetic effects of middle cerebral artery occlusion in the spontaneously hypertensive rat, Brain Res. 621 (1) (1993) 79–86.

[33] H.H. Chang, Y.C. Lee, M.F. Chen, J.S. Kuo, T.J. Lee, Sympathetic activation increases basilar arterial blood flow in normotensive but not hypertensive rats, Am. J. Physiol. Heart Circ. Physiol. 302 (5) (2012) H1123–H1130.
[34] M.C. Boguszewski, G. Johannsson, L.C. Fortes, Y.B. Sverrisdottir, Low birth size and final height predict high sympathetic nerve activity in adulthood, J. Hypertens. 22 (6) (2004) 1157–1163.
[35] I.J. Rg, C.D. Stehouwer, E.J. de Geus, M.M. van Weissenbruch, H.A. Delemarre-Van De Waal, D.I. Boomsma, Low birth weight is associated with increased sympathetic activity: dependence on genetic factors, Circulation 108 (5) (2003) 566–571.
[36] C.J. Petry, M.W. Dorling, C.L. Wang, D.B. Pawlak, S.E. Ozanne, Catecholamine levels and receptor expression in low protein rat offspring, Diabet. Med. 17 (12) (2000) 848–853.
[37] T. Hiraoka, T. Kudo, Y. Kishimoto, Catecholamines in experimentally growth-retarded rat fetus, Asia Oceania J. Obstet. Gynaecol. 17 (4) (1991) 341–348.
[38] C.T. Jones, J.S. Robinson, Studies on experimental growth retardation in sheep. Plasma catecholamines in fetuses with small placenta, J. Dev. Physiol. 5 (2) (1983) 77–87.
[39] G. Simonetta, A.K. Rourke, J.A. Owens, J.S. Robinson, I.C. McMillen, Impact of placental restriction on the development of the sympathoadrenal system, Pediatr. Res. 42 (6) (1997) 805–811.
[40] E.V. Rouwet, A.N. Tintu, M.W. Schellings, M. van Bilsen, E. Lutgens, L. Hofstra, et al., Hypoxia induces aortic hypertrophic growth, left ventricular dysfunction, and sympathetic hyperinnervation of peripheral arteries in the chick embryo, Circulation 105 (23) (2002) 2791–2796.
[41] K. Ruijtenbeek, F.A. le Noble, G.M. Janssen, C.G. Kessels, G.E. Fazzi, C.E. Blanco, et al., Chronic hypoxia stimulates periarterial sympathetic nerve development in chicken embryo, Circulation 102 (23) (2000) 2892–2897.
[42] J. Mamet, J. Peyronnet, J.C. Roux, D. Perrin, J.M. Cottet-Emard, J.M. Pequignot, et al., Long-term prenatal hypoxia alters maturation of adrenal medulla in rat, Pediatr. Res. 51 (2) (2002) 207–214.
[43] J. Atkinson, N. Trescases, C. Benedek, N. Boillat, A.K. Fouda, F. Krause, et al., Alpha-1 and alpha-2 adrenoceptor agonists induce vasoconstriction of the normotensive rat caudal artery in vitro by stimulation of a heterogeneous population of alpha-1 adrenoceptors, Naunyn Schmiedeberg's Arch. Pharmacol. 338 (5) (1988) 529–535.
[44] B. Wilffert, M.A. Gouw, P.B. Timmermans, P.A. van Zwieten, Interaction between beta 2-adrenoceptor-mediated vasodilation and alpha 1-adrenoceptor-mediated vasoconstriction in the pithed normotensive rat, J. Cardiovasc. Pharmacol. 5 (5) (1983) 829–835.
[45] D. Tripovic, A. Al Abed, N.M. Rummery, N.J. Johansen, E.M. McLachlan, J.A. Brock, Nerve-evoked constriction of rat tail veins is potentiated and venous diameter is reduced after chronic spinal cord transection, J. Neurotrauma 28 (5) (2011) 821–829.
[46] J.D. Raffetto, X. Qiao, K.G. Beauregard, A.F. Tanbe, A. Kumar, V. Mam, et al., Functional adaptation of venous smooth muscle response to vasoconstriction in proximal, distal, and varix segments of varicose veins, J. Vasc. Surg. 51 (4) (2010) 962–971.
[47] M.J. Meldrum, C.S. Xue, L. Badino, T.C. Westfall, Angiotensin facilitation of noradrenergic neurotransmission in central tissues of the rat: effects of sodium restriction, J. Cardiovasc. Pharmacol. 6 (6) (1984) 989–995.
[48] S. Guimaraes, H. Pinheiro, P. Tavares, A. Loio, D. Moura, Differential effects of eprosartan and losartan at prejunctional angiotensin II receptors, Naunyn Schmiedeberg's Arch. Pharmacol. 363 (5) (2001) 509–514.
[49] M.F. Lokhandwala, E. Amelang, J.P. Buckley, Facilitation of cardiac sympathetic function by angiotensin II: role of presynaptic angiotensin receptors, Eur. J. Pharmacol. 52 (3–4) (1978) 405–409.
[50] S.M. Arribas, M.J. Alonso, J. Marin, F. Fernandes, J.L. Llergo, C.F. Sanchez-Ferrer, et al., Noradrenergic transmission in the tail artery of hypertensive rats transgenic for the mouse renin gene Ren-2, J. Auton. Pharmacol. 16 (2) (1996) 69–77.
[51] M. Morato, D. Pinho, T. Sousa, S. Guimaraes, D. Moura, A. Albino-Teixeira, Pre- and postjunctional effects of angiotensin II in hypertension due to adenosine receptor blockade, Eur. J. Pharmacol. 531 (1–3) (2006) 209–216.
[52] R.R. Singh, L.A. Cullen-McEwen, M.M. Kett, W.M. Boon, J. Dowling, J.F. Bertram, et al., Prenatal corticosterone exposure results in altered AT1/AT2, nephron deficit and hypertension in the rat offspring, J. Physiol. 579 (2007) 503–513 Pt 2.
[53] P. Pladys, I. Lahaie, G. Cambonie, G. Thibault, N.L. Le, D. Abran, et al., Role of brain and peripheral angiotensin II in hypertension and altered arterial baroreflex programmed during fetal life in rat, Pediatr. Res. 55 (6) (2004) 1042–1049.
[54] C. Mao, H. Zhang, D. Xiao, L. Zhu, Y. Ding, Y. Zhang, et al., Perinatal nicotine exposure alters AT 1 and AT 2 receptor expression pattern in the brain of fetal and offspring rats, Brain Res. 1243 (2008) 47–52.
[55] P.Y. Gutiérrez-Arzapalo, P. Rodríguez-Rodríguez, D. Ramiro-Cortijo, Á.L. López De Pablo, M.R. López-Giménez, L. Condezo-Hoyos, et al., Role of fetal nutrient restriction and postnatal catch-up growth on structural and mechanical alterations of rat aorta, J. Physiol. (2017), https://doi.org/10.1113/JP275030.